

# The future of power generation in Brazil: An analysis of alternatives to Amazonian hydropower development



Felipe A.M. de Faria, Paulina Jaramillo \*

Department of Engineering & Public Policy, Carnegie Mellon University, 5000 Forbes Avenue, Pittsburgh, Pennsylvania 15213, United States

## ARTICLE INFO

### Article history:

Received 12 January 2017

Revised 1 August 2017

Accepted 5 August 2017

Available online 23 August 2017

### Keywords:

Stochastic dual dynamic programming

Brazilian power system

Impact assessment

## ABSTRACT

The Brazilian government has plans to build 26 large hydropower plants in the Amazon basin between 2013 and 2028. These plants will have a total installed capacity of 44 GW, 9000 km<sup>2</sup> of reservoir area, and a total cost of US\$ 30–70 billion. In this paper we aim to evaluate alternative generation pathways to avoid the adverse social and environmental impacts associated with reservoirs in the Amazon. Specifically we model the Brazilian electricity network under five capacity expansion scenarios. We assumed the government expansion plans as the baseline and created alternative scenarios where wind and natural gas power plants replace large Amazonian hydropower plants. We compared the scenarios using several performance indicators: greenhouse gas emissions, land use, capital and operational costs, wind curtailments, and energy storage in the hydropower reservoirs. The simulations suggest that a more aggressive policy towards wind generation than the baseline has the potential to replace Amazon hydropower providing advantages to the system operation (e.g., higher storage in hydropower reservoirs). However, when installed wind capacity reaches 24% to 28% of the total installed capacity, more thermal generation is required to balance the hydro-wind variability, increasing the operational costs and greenhouse gas emissions compared to the baseline.

© 2017 International Energy Initiative. Published by Elsevier Inc. All rights reserved.

## Introduction

Since the middle of the 20th century, Brazil has supplied most of its electricity demand by building large hydropower plants. Currently, hydropower plants larger than 30 MW comprise 61% of the total installed system capacity of 124 GW (Agencia Nacional de Energia Eletrica (Brazilian Electricity Agency), 2015). Recently, the construction of new hydropower plants has been concentrated in the Amazon basin, where large plants like Jirau (3,750 MW), Santo Antônio (3,150 MW), and Belo Monte (11,200 MW) were recently built. Large-scale hydropower expansion has been taking place in the Amazon region because most of the hydropower potential of other regions has already been exploited. In addition to the previously listed projects, there are several projects currently under construction, such as Teles Pires (1,820 MW), São Manoel (746 MW) and Sinop (461 MW). This expansion will continue as the government indicates that most of proposed hydropower projects in the country will be built in the Amazon (e.g. São Luis do Tapajos (6,133 MW), São Simão Alto (3,509 MW)) (MME and EPE, 2014).

Although hydropower has been seen as the main supply source to meet the growing demand for electricity, projects located in the Amazon could have significant environmental and social impacts (Fearnside, 2005; Fearnside, 2001; da Silva Soito and Freitas, 2011; Latrubesse et al., 2017.). The reservoirs in recent and announced reservoirs in the Amazon would flood 9,000 km<sup>2</sup> (out of an area of roughly 5 million km<sup>2</sup> in the Legal Amazon region in Brazil), which can adversely affect flora, fauna, and ecosystem services. The dam also blocks the natural river flow, affecting the migration of aquatic species and resulting in changes in the oxygen, thermal, and sedimentary conditions in the reservoir area and downstream (Tundisi et al., 1993; Tundisi and Rocha, 1998; Friedl and Wuest, 2002). In some cases, the flooding and decay of large stocks of biomass in the reservoir area lead to greenhouse gas emissions that are comparable to those from fossil fuel power plants (de Faria et al., 2015; dos Santos et al., 2006; Fearnside, 2015). Furthermore, large hydropower projects also affect the local population through the resettlement of people living in the reservoir areas and the deterioration of social cohesion because of the high influx of workers (Jackson and Sleigh, 2000; Tilt et al., 2009), and loss of agricultural production.

In this paper we develop different capacity expansion scenarios for the Brazilian power system in order to compare the costs and benefits of power plants in the Brazilian Amazon against other alternatives for

\* Corresponding author.

E-mail address: paulina@cmu.edu (P. Jaramillo).

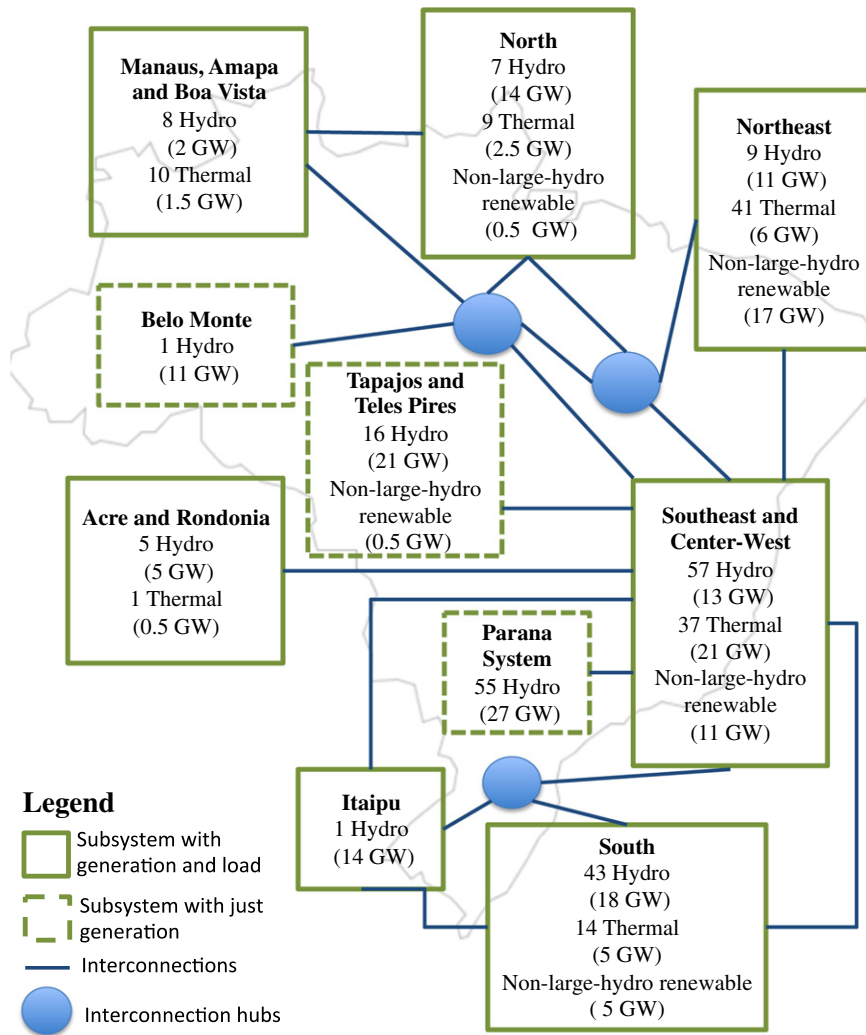


**Fig. 1.** Brazilian integrated system scheme with government forecasted capacity by 2028. Non-large-hydro renewables include wind, small hydropower plants (<30 MW), and biomass. Source: Authors' construction using data from EPE (EPE, 2015).

power generation. We simulate the electric system operations in order to estimate performance indicators such electricity production and operational costs, quantity of stored energy in the reservoirs, wind curtailments,<sup>1</sup> and greenhouse gas (GHG) emissions across the different scenarios. The alternative scenarios include replacing Amazonian hydropower capacity with wind power in the Northeast and South regions, or natural gas plants in the Southeast.

**Data and methods**

*Current system characteristics and general description of alternative scenarios*

The Brazilian electricity network is an interconnected system of 10 subs-regions: 1) North, 2) Northeast, 3) Southeast, 4) South, 5) Paraná, 6) Itaipu, 7) Teles Pires and Tapajós, 8) Belo Monte, 9) Acre and Roraima, and 10) Manaus, Amapá and Boa Vista. Some of these sub-systems contain power plants and loads (e.g. Southeast), but others contain just generation (e.g. Belo Monte). Fig. 1 describes a scheme of the sub-systems and their major interconnections.

The Empresa de Pesquisa Energetica (EPE) is the Brazilian state company responsible for creating the country's long-term energy plans (including plans for the power sector, as well as the natural gas, oil sectors). Every year EPE issues an expansion plan for the power sector (Plano Decenal de Energia, in Portuguese), which includes a set of files containing the detailed power plant characteristics used to model system operations and forecast changes in the system (EPE, 2015). As part of this expansion plan, EPE provides detailed data for each power plant, including water flows, reservoir limits, fuel types for thermal plants, minimum and maximum capacity, among others. Table S1 in the supporting information includes a full list of available variables for each power plant. In this paper, we rely on the data from the EPE report released in January 2015 (hereafter the 2015 EPE report files), which focused on modelling the system between 2013 and 2023, but provided data up to 2028. We used 2015 EPE report files as the reference scenario (baseline) to represent the electricity system between 2013 and 2028. Table 1 summarizes annual capacity additions by fuel type in the baseline. In addition, Table S5 in the supporting information includes detailed information about each hydropower plant to be constructed by 2028 in this baseline scenario. While plans for some of the power plants may be abandoned, we assume that all of them will be available following the proposed schedule included in the EPE report. Finally, we note that the EPE data include information for each hydro and thermal power plant in the fleet, while aggregate

<sup>1</sup> Wind curtailments are defined as “a reduction in the output of a generator from what it could otherwise produce given available resources.” (Bird et al., 2014)

**Table 1**  
Initial installed capacity, annual capacity additions, and final installed capacity by fuel type.

Year	All scenarios	Capacity information in baseline			Capacity information in Wind27			Capacity information in Wind39 and Coal/Oil/Diesel Retirements <sup>a</sup>			Capacity information in Natural Gas		
	Non- Amazon hydro	Amazon hydro	Thermal	Wind	Amazon hydro	Thermal	Wind	Amazon hydro	Thermal	Wind	Amazon hydro	Thermal	Wind
Total installed capacity in May 2013 (MW)	76,259	9,927	20,170	6,848	9,927	20,170	6,848	9,927	20,170	6,848	9,927	20,170	6,848
Annual capacity additions (MW)													
2013	422	1,203	2,925	0	1,203	2,925	0	0	2,925	1,500	1,203	2,925	0
2014	111	2,605	1,343	0	2,605	1,343	0	0	1,343	3,000	2,605	1,343	0
2015	0	4,554	1,102	3,750	4,554	1,102	3,750	0	1,102	9,750	4,554	1,102	3,750
2016	674	4,570	0	3,000	4,570	0	3,000	0	0	9,000	4,570	0	3,000
2017	45	3,886	316	1,500	3,886	316	1,500	0	316	6,000	3,886	316	1,500
2018	45	4,767	1,705	1,500	4,767	1,705	1,500	0	1,705	7,500	4,767	1,705	1,500
2019	328	611	0	1,500	611	0	1,500	0	0	2,250	611	0	1,500
2020	1,018	945	0	750	0	0	1,500	0	0	1,500	0	567	750
2021	290	2,533	0	750	0	0	3,750	0	0	3,750	0	1,520	750
2022	619	2,155	0	750	0	0	3,000	0	0	3,000	0	1,293	750
2023	819	2,419	0	1,500	0	0	3,750	0	0	3,750	0	1,451	1,500
2024	1,292	4,235	0	1,500	0	0	6,000	0	0	6,000	0	2,541	1,500
2025	347	4,818	1,000	2,250	0	1,000	7,500	0	1,000	7,500	0	3,891	2,250
2026	567	2,801	0	2,250	0	0	5,250	0	0	5,250	0	1,680	2,250
2027	1,135	2,326	1,300	3,000	0	1,300	5,250	0	1,300	5,250	0	2,696	3,000
2028	948	1,821	10,300	2,250	0	10,300	4,500	0	10,300	4,500	0	11,393	2,250
Total additions between 2013 and 2028 (MW)	8,660	46,249	19,991	26,250	22,196	19,991	51,750	0	19,991	79,500	22,196	34,423	26,250
Total installed capacity in 2028 (MW)	84,919	56,176	40,161	33,098	32,123	40,161	58,598	9927	40,161	86,348	32,123	54,593	33,098

<sup>a</sup> Total changes in thermal capacity in the Wind39 and Coal/Oil/Diesel (COD) retirement are the same, but the type of fuel used differs in the two scenarios. In the Wind39 scenario, we relied on thermal power plants additions reported in the EPE (Table S3 in the supporting information). In the COD scenario, natural gas provides all fossil thermal energy.

data at the sub-system level are provided for other non-large hydro renewables such as wind, small hydropower plants, and biomass (Fig. S2 in the supporting information).

The objective of this paper is to compare different electricity generation expansion scenarios for the Brazilian integrated electric system using performance indicators that characterize the technical, economic, and environmental features of each scenario. Specifically, we aim to evaluate alternatives to hydroelectric expansion in the Brazilian Amazon. We thus developed four alternative scenarios that include varying levels of wind and thermal power capacity. Table 1 summarizes initial installed capacity, annual capacity additions, and final installed capacity by fuel type in these scenarios. The criteria for the alternative scenarios we developed was that the average annual generation from the alternative resources would match the average hydro generation from the Amazonian hydropower plants they are meant to replace, based on the average capacity factor of the different resources. If this approximation resulted in excess generation (curtailment), we parametrically reduced installed wind/natural gas capacity until the simulations resulted in similar levels of lost-load between the alternative scenarios and the baseline. The supporting information includes a more detailed description of the process we used to estimate new capacity installations.

1. Scenario “Wind27”: Replaces hydroelectric power plants scheduled to start-up in the Amazon after 2020 with wind farms, so that by 2028 wind power accounts for 27% of total installed capacity.
2. Scenario “Wind39”: Replaces hydroelectric power plants scheduled to start-up in the Amazon after 2013 with wind farms, so that by 2028 wind power accounts for 39% of the total installed capacity.
3. Scenario “Natural Gas”: Replaces hydroelectric power plants scheduled to start-up in the Amazon after 2020 with natural gas combined-cycle (NGCC) power plants located in the Southeast.
4. Scenario “Coal/Oil/Diesel (COD) retirement”: Assumes the same conditions detailed in the “Wind39” scenario, but also assumes that natural gas power plants replace all current and future coal, oil, and diesel power plants.

#### Power system model

In order to model the optimal generation scheduling of the power plants in the Brazilian system under the different scenarios, we relied on SDDP (stochastic dual dynamic programming), which is a commercial dispatch model that has been used in the past to model the Brazilian power system (Gorenstin et al., 2004). The model calculates the least-cost stochastic operating schedule of the system, taking into account operational details of the plants such as water inflows and operational limits, as well as the variability of non-hydro renewable resources like wind (Gorenstin et al., 2004; Pereira and Pinto, 1991; PSR, 2014). SDDP represents energy transfer limits between neighbouring systems aggregating energy by sub-regions. In this case it is necessary to define a load supply equation for each sub-region. We populated SDDP using the power plant and load data from the 2015 EPE report files. For the alternative scenarios we modified these files to include new natural gas or wind plants as described in the scenario description in the previous section.

In purely thermal systems, the operation costs of each plant largely depend on its fuel cost. Thus, the system operator would first dispatch the plants with the lower fuel costs. However, the operation of systems with a lot of hydropower is more complex because the system operator must continuously decide whether to save or use water from the reservoirs. If the operator decides to use hydro energy today, and future inflows are high (allowing for reservoir storage recovery), system operations will be efficient (i.e. less wasted energy) (PSR, 2014). In contrast, if a drought occurs, it may be necessary to use more expensive thermal generation in the future, or even shed load. Similarly, if storage levels are kept high through more use of thermal today, and high inflows occur in the future, reservoirs may spill, which results in waste of energy and higher operational costs. If a drought occurs instead, storage displaces thermal generation and the system operates efficiently (PSR, 2014). The problem is stochastic because water inflow to the reservoirs is a result of a random process and it is impossible to have a perfect forecast of future inflows (Gorenstin et al., 2004). Additionally, most inflow sequences are serially correlated (PSR, 2014). In other words, if the

inflow of the past month was wetter than the average, there is a tendency that the inflows in the next few months will be wetter too.

The SDDP application in this paper allows for the comparison of different expansion plans taking into account the hydropower-scheduling problem. SDDP determines the sequence of hydro releases, which minimizes the expected thermal operation costs (given by fuel costs and penalties for rationing) during the planning horizon (Pereira and Pinto, 1991; PSR, 2014). The model treats the output of non-large-hydro renewable resources, like wind, as a negative load with zero cost. The SDDP algorithm decomposes the multi-stage stochastic problem into several one-stage sub-problems. Each sub-problem corresponds to a linearized optimal power flow with additional constraints representing the hydro reservoir equations and a piecewise linear approximation of the expected future cost function (Pereira and Pinto, 1991). For a given stage of the problem, the future cost is a function of the reservoir storage levels and inflows. SDDP incorporates the stochastic characteristic of inflows by solving the optimization problem several times (Monte Carlo simulation). For this paper we solve the optimization for each scenario using 400 simulations. The algorithm also incorporates serial autocorrelation of inflows by modeling the water inflows to the reservoirs using an autoregressive linear regression model based on the historical monthly inflows for each hydropower reservoir. The supporting information contains more details about the hydropower scheduling problem and the SDDP algorithm.

#### Modeling wind output

Variability and intermittency of wind power adds new constraints for system operations, particularly as the power system reaches larger penetrations of this resource (Apt and Jaramillo, 2014). The EPE's database limits the ability to model these additional constraints in the power system model as the database currently reports aggregate values for non-hydro renewables at the sub-system level. Moreover, the data only include a constant monthly output from these resources for each sub-system, as shown in Fig. S2 in the supporting information. As a result, the available EPE data do not account for the stochasticity of wind speed and associated variability in power output.

To overcome this issue, we created wind generation series for current and future hypothetical wind farms in Brazil using wind speed data from the U.S. National Centers for Environmental Prediction (NCEP) Climate Forecast System Reanalysis (CFSR) (Saha et al., 2016). NCEP-CFSR is an atmospheric reanalysis product available at an hourly time resolution from 1979 to the present and a horizontal resolution of  $0.5^\circ$  latitude  $\times$   $0.5^\circ$  longitude. Reanalysis data are attractive for wind power studies because they can offer wind speed data for large areas and long time periods in locations where historical data are not available (Rose and Apt, 2015). We evaluated the validity of using CFSR wind speeds to generate wind power output series using real data from 32 wind farms in Brazil. The supporting information details this validation analysis.

To model new wind (beyond what is already available in the system or reported to start operations by 2020), we created groups of 25 hypothetical wind farms of 30 MW of installed capacity each. Thus, each group has 750 MW of installed capacity. To enable the use of CFSR data, we modeled the location of new wind farms using a lottery with replacement for each wind farm in each group. This lottery is based on a sample of 1065 wind farms that are in the early stages of licensing in the northeastern and southern states (see Fig. S3 in the supporting information).

After identifying the location of each existing and hypothetical wind farm, we created wind energy generation series by simulating the energy output from each existing and hypothetical wind farm using the NCEP-CFSR hourly wind speeds during the 1979–2010 period. We then aggregated the results for the 25 wind farms within each group by month and load level (our study relies on 3 load levels to simulate demand for electricity, as described below). As a result, each group of

750 MW wind farms contains 96 monthly series of plant capacity factors (32 for each load level), which are inputs to SDDP. SDDP draws a lottery from those monthly series and optimizes the hydro and thermoelectric power plant schedule according to the wind energy output from the selected series. Because of the reservoir storage constraints, SDDP may choose to curtail wind output below the simulated capacity factors. However, such curtailment represents wasted energy and should be avoided.

#### Demand and interconnection representation

The EPE database reports electricity demand in a typical day in the Brazilian system using three load levels within each month (stage): high, medium, and low. EPE projects future electricity demand based on demographic, economic, and sectorial studies about residential and industrial electricity consumption (EPE, 2014). In so much as meteorological variable influence the shape of the load curve in each month, those factors are accounted for in the EPE projects, and as a result these load profiles should capture correlation with wind profiles driven by meteorological conditions. However, a thorough analysis of this correlation is beyond the scope of this paper.

The loads EPE provides are defined for each sub-system (EPE, 2015) so that three pairs of duration (hours) and demand (GWh) by month represent each load level, and thus capture within-day variability of demand for electricity. According to the EPE, in a typical day the high load occurs between 6 pm and 9 pm; the low load occurs from midnight am to 7 AM; and the rest of hours of the day are considered medium load (ONS, 2010). SDDP relies on these load curves as a constraint to optimize system operations. For our analysis, all scenarios have the same demand profile. Fig. 2 shows the annual load duration curves (built based on the monthly data for each load level) in 2014 and 2028.

Fig. 1 shows the transmission links between sub-systems in the Brazilian power system (the figure does not show transmission lines within each sub-region). In order to account for the transmission system in SDDP, transmission plans and costs for the alternatives scenarios needs to be available at the sub-system level. Since such disaggregated data are not available, our model does not include transmission constraints. Thus, our analysis can be seen as an optimistic representation of system operations that do not account for inefficient power plant dispatch that may result from transmission constraints, which is a common limitation in other power system research (Oates and Jaramillo, 2013).

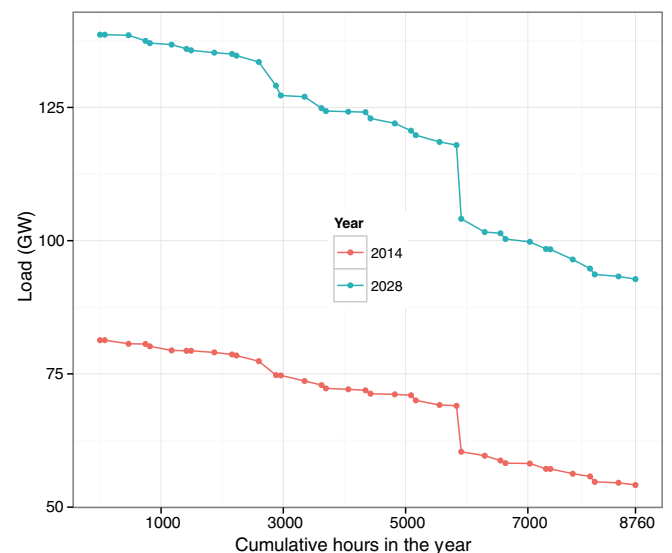


Fig. 2. Load duration curves for 2014 and 2028, requirements and capacity utilization.

## Performance indicators

In order to compare the baseline and the alternative scenarios, we used a set of performance indicators that include electricity generated by fuel type; land use and greenhouse gas emissions; investment and operations costs; water storage levels; and wind curtailments. Electricity generation by fuel type is the result of optimal dispatch of the power plant fleet of each scenario. To evaluate the performance of the hydropower plants in each scenario, we also compared the energy storage levels in the hydroelectric reservoir, which is a measure of the system resilience against droughts. This value is calculated using the volume of water stored in each reservoir with storage capacity multiplied by its average production coefficient ( $\text{MWh}/\text{m}^3$ ). Further, we used wind curtailment levels (in megawatt-hour of wind power) and lost load as indicators of system performance. The lost load is defined by the ratio (in percentages) between the energy (in GWh) that the system was not able to supply to satisfy the demand and the total demand (in GWh).

The optimization in SDDP does not account for the capital costs of new power plants associated with each scenario. In order to estimate total investment costs, we rely on a database from The Chamber of Electric Energy Trading (*Câmara de Comercialização de Energia - CCEE*, in Portuguese), which is the Brazilian electricity market operator. The database includes all new power plants that sold energy in public capacity auction between 2005 and 2015 (CCEE, 2015). For each of 826 plants included, the database provides the installed capacity and the forecasted capital costs. We relied on these data to estimate the costs of building new power plants in our expansion scenarios. The supporting information contains a detailed description of the CCEE data.

System-level operating costs are an output of the SDDP, based on the assumption about operating costs for individual power plants. The EPE database provides the operation costs for each thermal power plant in the baseline scenario, which vary from 20 to 1,000 reais per MWh (6 to 303 U.S. dollars per  $\text{MWh}^2$ ). The Brazilian government controls gas prices and we assumed the same operational costs defined by EPE of 250 reais/MWh (70 US\$/MWh) for the new natural gas power plants. Wind farms have no variable operating costs in this model, as they do not rely on commodity fuels. Wind and hydropower plants annual O&M costs are estimated to be 2% of the total construction costs. We annualized the capital and O&M costs by assuming that new power plants have a lifetime of 50 years and discount rate of 12%. The supporting information contains more details about cost calculations.

Direct and indirect land transformation requirements (excluding transmission lines) serve as a proxy for environmental impacts like habitat fragmentation and disruption of ecosystems. To estimate the direct land use transformation for hydropower development, we relied on the reported reservoir area of all the projects in the EPE schedule. To estimate the direct land transformation for wind power and thermal power plants, we relied on values reported in the literature (Denholm et al., 2009; Fthenakis and Kim, 2009). Indirect land transformation from hydropower, wind, and natural gas are also estimated using the life cycle assessment literature (Fthenakis and Kim, 2009). The supporting information contains the details about land use rates applied to this study.

Due to growing efforts by the international community to reduce global greenhouse gas (GHG) emissions that contribute to climate change, GHG emissions associated with our capacity expansion scenarios are a relevant metric of comparison. GHG emissions from hydropower are usually low, however, reservoirs located in tropical forested areas have the potential to emit large quantities of methane ( $\text{CH}_4$ ), a more powerful GHG gas compared to carbon dioxide ( $\text{CH}_4$ ) (Barros et al., 2011).  $\text{CO}_2$  and  $\text{CH}_4$  emissions from hydropower result

from the oxic/anoxic decomposition of the flooded organic matter from different sources within the reservoir (e.g. vegetation and soils) and from outside the reservoir (e.g. sedimentary organic matter input from the upstream river basin). Estimates for eighteen new hydropower plants planned in the Amazon indicate total emissions that vary between 9 and 21 Tg of  $\text{CH}_4$  and 81–310 Tg of  $\text{CO}_2$  over a hundred years (de Faria et al., 2015). Based on the average, lower, and upper bounds values defined by de Faria et al. (2015), we estimated the emissions from eighteen major Amazon reservoirs in the baseline scenario (Belo Monte, Bem Querer, Cachoeira do Caí, Cachoeira do Caldeirão, Cachoeira dos Patos, Colider, Ferreira Gomes, Jamanxim, Jatobá, Jirau, Marabá, Salto Augusto de Baixo, Santo Antônio, São Luís do Tapajos, São Manoel, Sao Simao Alto, Sinop, and Teles Pires) over the first 15 years of operation and using a 100-year global warming potential for  $\text{CH}_4$  equal to 34, which is the updated GWP in the 5th Assessment Report of the Intergovernmental Panel for Climate Change (I.P.O.C.C. IPCC, 2014). We also calculated GHG emissions from thermal power plants including nuclear. These values are the median estimates reported by the (IPCC) (Moomaw et al., 2011): nuclear (16 g  $\text{CO}_2\text{e}/\text{kWh}$ ), oil/diesel (840 g  $\text{CO}_2\text{e}/\text{kWh}$ ), natural gas (470g $\text{CO}_2\text{e} /\text{kWh}$ ), biomass (470 g  $\text{CO}_2\text{e} /\text{kWh}$ ), and coal (1,000 g  $\text{CO}_2\text{e} /\text{kWh}$ ).

## Results and discussion

### Generation output projections

Fig. 3 describes the optimal generation output by fuel type and load level for the initial conditions in 2014 and the final conditions for each scenario in 2028. The lines in Fig. 3 represent the average generation output per month considering 400 simulations of the optimal system operation for each scenario. The initial conditions in 2014 represent the system operation before any significant additional capacity and is very similar across all scenarios.

The initial conditions in 2014 (first column in Fig. 3) show that hydropower generation is the major source of electricity. Hydropower accounts, on average, for 75% of the total electricity produced in 2014. The variability in hydropower output across the load levels (represented by the different line colours: red - high, blue - medium, and green - low) indicates that hydropower is dispatched to meet the within-day variability. In contrast, thermal power plants are operated as base-load. Thermal generation accounts for 15% of the total electricity generation in 2014, while wind energy accounts for only 5% of the total electricity generation. Other non-large hydro renewables like biomass, small hydropower plants, and solar generation accounts for 5% of generation but they are not represented in Fig. 3 because they are similar for all scenarios.

In the baseline, 46 GW of new hydropower plants in the Amazon fulfil most of the additional capacity requirements between 2014 and 2028. In 2028, average hydropower generation accounts for 68% of the total generation, a reduction from the initial condition. Thermal generation decreases to 13% of generation in 2028, and wind generation increases to 12% of total generation. Other non-large-hydro renewables account for 7% of total generation. Thus, the baseline results indicate slightly higher levels of non-large-hydro renewable generation throughout the study horizon and a reduction of thermal generation compared to the initial conditions. Note, however, that thermal generation in 2028 varies by load level indicating that these plants are dispatched to meet within-day and seasonal wind variability, which increases throughout the analysis period.

The major difference between the “Wind27” and the baseline scenarios is the higher penetration of wind in the system after 2020. In 2028, while total renewable generation (including hydro, wind, solar, and other renewables) continues to account for 85% of total generation in the “Wind27” scenario (wind is 27% of the total installed capacity), the contribution of wind power increases to 20% of total generation. Most of the new wind plants are located in the Northeast subsystem

<sup>2</sup> We use the foreign exchange rate for May 2016 (1 US dollar = 3.33 Reais).

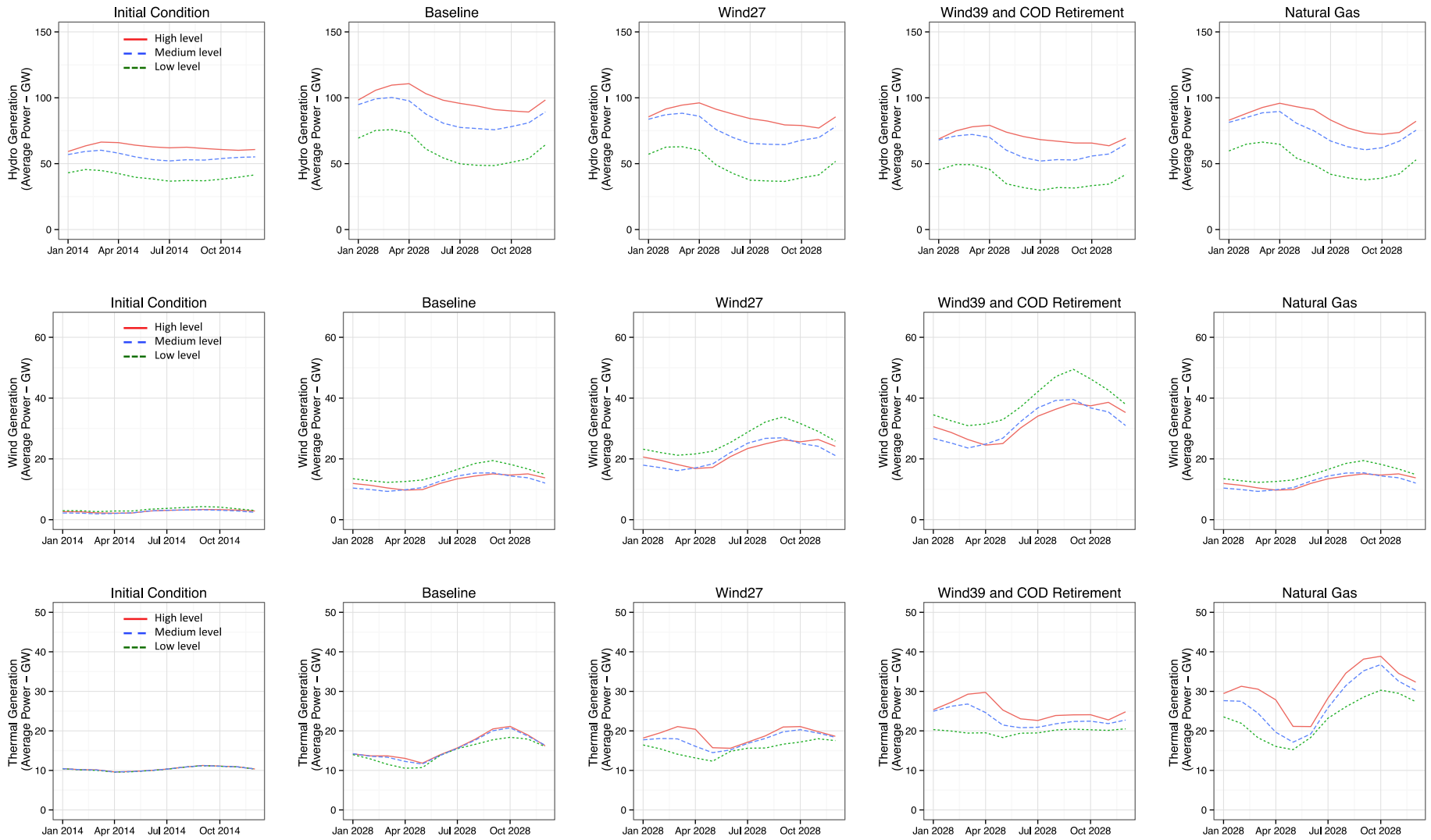


Fig. 3. Average optimal dispatch for each scenario by source (wind, hydro and thermal power plants) and by load level (high, medium, load).

where higher wind speeds occur from July to November. These higher wind speeds occur as the dry season begins in July/August (when hydropower output decreases). By 2025, wind accounts for 24% of installed capacity and thermal generation starts to vary significantly by demand block to manage intra-day variability in net load (load minus non-large hydro renewables), and by season to balance hydro-wind variability (see Fig. S9 in the supporting information). Furthermore, because wind speeds are higher during low-load periods, thermal power output increases during periods of higher demand in this scenario.

The “Wind39” scenario represents a more aggressive policy towards wind generation. It characterizes an expansion scenario where wind replaces all 46 GW of recently built, under construction, and future hydropower plants in the Amazon. In this scenario, wind power replaces large power plants in the Amazon like Jirau, Santo Antonio, and Belo Monte while thermal generation decreases and continues to be dispatched as base load up to 2018. By 2020, wind accounts for 28% of total installed capacity, and thermal power plants start being dispatched to meet high and medium demand periods during the low wind speed season (February–June). Between 2020 and 2028 (See Fig. S9 in the supporting information), average thermal generation in the “Wind39” scenario also increases faster compared to the baseline and the “Wind27” scenarios. In December 2028, thermal, wind, and total renewable generation account, on average, for 19%, 30% and 84% of the total electricity generated in the system, respectively. Thus, increasing the participation of wind to replace hydropower leads to a higher output from thermal power plants used to balance within-day and seasonal variability from wind plants compared to the baseline and the “Wind27” scenarios. The average dispatch profile for the “COD retirement” scenario is similar to that of the “Wind39” scenario.

In the “Natural Gas” scenario, natural gas power plants (rather than wind) replace the same hydropower plants as in the “Wind27” scenario. Increases in wind capacity in this scenario follow the schedule of the baseline scenario. The lack of significant additional capacity from hydro or wind power plants in this scenario increases the average output from thermal generation. After 2024, the seasonal variability in thermal generation also increases to compensate for the seasonal changes in hydropower output from existing resources. In 2028, when wind power accounts on average for 12% of the total installed capacity, thermal generation accounts for 23% of total generation. This scenario has the lowest share of renewable output (including hydro) across all scenarios.

#### Reservoir storage

Energy storage provided by storing water in hydropower reservoirs adds resiliency against droughts as well as system flexibility. Fig. 4 shows the energy stored in hydropower reservoirs in 2014 (initial condition) and in 2028, measured as a total system storage capacity in TWh. Note that this figure shows the average of 400 simulations for each expansion scenario over the period of analysis. For a given month, the energy storage is defined by the multiplication of the volume of stored water in each reservoir by its average production coefficient (MWh per m<sup>3</sup> of water). The dry and wet seasons explain the valleys and peaks in the average energy storage profile in Fig. 4. During the wet season, inflows tend to be above the annual average and the system operator manages the power plant dispatch to fill the storage reservoirs. On the other hand, inflows are below the annual average in the dry season, but the operator can use stored water from the reservoir

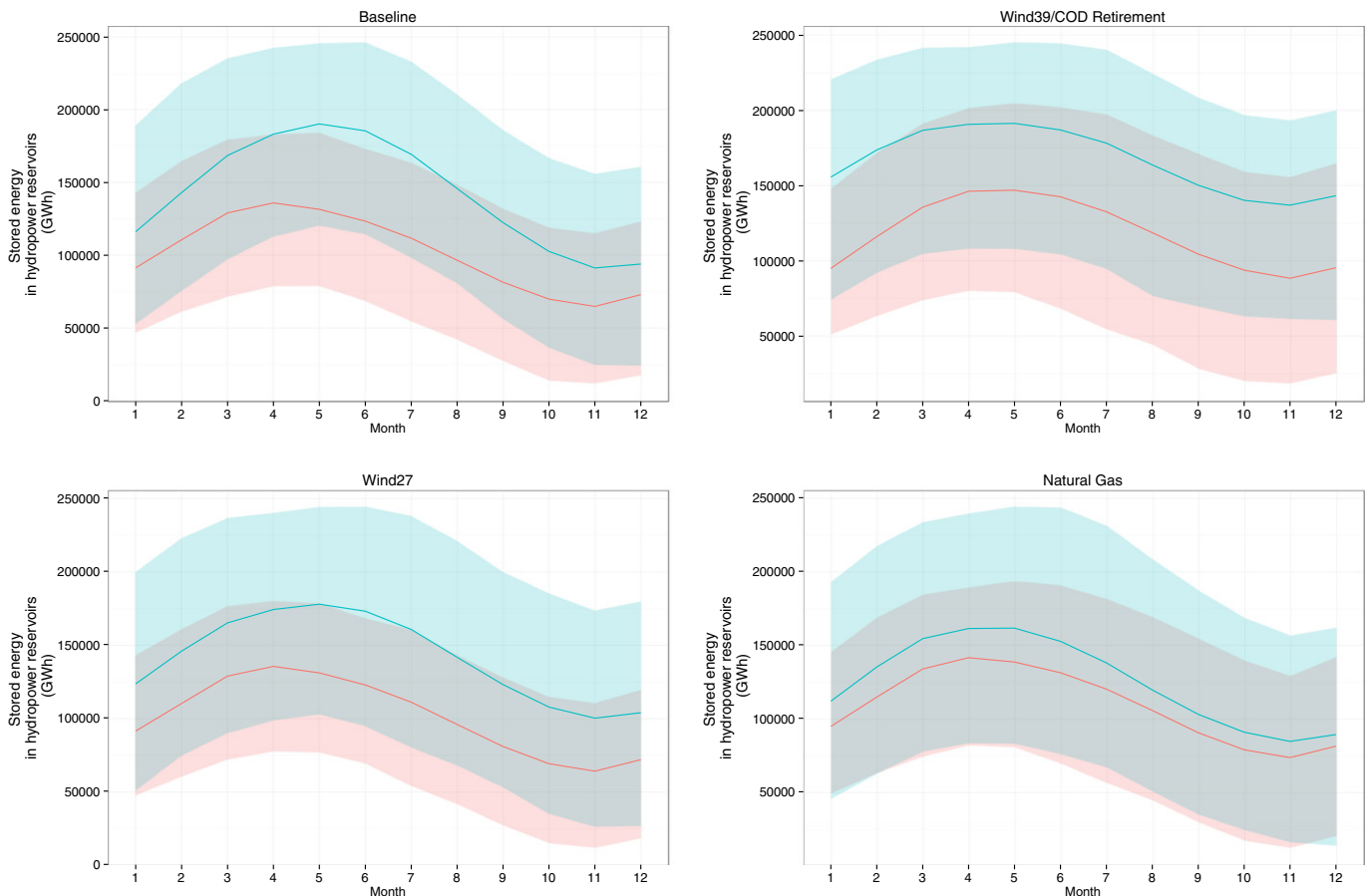


**Fig. 4.** Average (lines) storage capacity in hydropower reservoir for each scenario presented in terms stored energy (GWh). Red: Year 2014; Green: Year 2028. The shades represent the 95% confidence interval from 400 hundred simulation for each scenario. “Coil/Oil/Diesel retirement” scenario has the same storage profiles as the “wind39” scenario.

to increase hydropower production to displace thermal generation. For example, in 2014 the average storage levels peak and trough happen in April (130 TWh) and November (65 TWh), respectively. Therefore, the average seasonal difference in storage levels was around 65 TWh of stored capacity.

Fig. 4 also accounts for the stochastic nature of reservoir inflows and wind speeds over time. The model captures the variability of this stochastic process by simulating each expansion plan over the study horizon 400 times using different inflows series and sampling different wind speed scenarios. As a result, SDDP output contains a distribution of the optimal dispatch under those 400 simulated conditions. The shading in Fig. 4 defines the 95% confidence interval (CI) for energy storage from the 400 simulated operations. For instance, the average storage level in April 2014 is 130 TWh but our simulation sample shows that storage level in April can vary from 75 to 180 TWh of storage (95% CI) depending on inflow and wind speed conditions.

The new hydropower power plants in the baseline scenario increase the average storage capacity in 2028 compared to the initial conditions in 2014. In 2028, baseline average storage peak occurs in May (185 TWh) indicating a peak shift of one month compared to the 2014 average level. This shift happens because the wet season in most of the new Amazon reservoirs happens between November and March. The 2028 baseline trough occurs in November (95 TWh) leading to an average seasonal difference of 90 TWh of stored capacity. This increase in the average seasonal difference in the baseline (2028) and the initial condition (2014) is a result of the greater seasonal variability from the operations of the large planned run-of-river hydropower plants in the Amazon, which are not accompanied by a proportional increase in storage capacity. These run-of-river designs aim to reduce the reservoir area (and volume) in order to mitigate environmental and social impacts from the reservoir creation, at the cost of no storage capacity. Additional storage capacity from Amazon dams corresponds to only 8% of the total storage capacity in 2013. Furthermore, there is an increase in the storage variance described by the 95% CI. For example, in April 2028 baseline storage levels vary from 125 to 245 TWh, which is a higher range compared to the initial conditions in 2014 (75 to 180 TWh).

The replacement of Amazonian hydropower by wind power plants has two major consequences for energy storage. First, there is a reduction in the average storage variability between wet and dry seasons because of the negative correlation between wind and water inflows (See Fig. 3). In 2028, the peak and trough for average storage levels in the “Wind27” happen in May (175 TWh) and November (100 TWh), respectively, representing an average seasonal difference of 75 TWh. In the case of the “Wind39” and “COD retirement” scenarios, the peak and trough for the average storage levels also happen in May (190 TWh of the storage capacity) and November (140 TWh of the storage capacity), respectively, representing an average seasonal difference of only 50 TWh.

Second, replacing Amazon hydropower plants with wind power slightly increases the variance in energy storage across simulations in each scenario because of the stochastic features of wind/inflows. This characteristic is clear in the “Wind27” and “Wind39” scenarios where the shades are “thicker” than in the baseline. In May 2028, for instance, storage levels may vary from 100 to 245 TWh for the “Wind27” scenario and from 110 to 245 TWh for the “Wind39” scenario, which are higher ranges compared to the baseline. Thus, increasing wind power participation in the Brazilian system increases the average percent storage but also increases the storage variance. Higher confidence intervals for the storage levels represent higher uncertainty in system operation costs because the system operator faced larger uncertainty about the conditions of the system in the future.

Finally, replacing Amazonian hydro with natural gas plants (Natural Gas scenario) reduces the system’s average capacity to store water and increases the storage variance compared to the baseline scenario. The thicker shade in Fig. 4 for the “Natural Gas” scenario represents the highest variance in storage levels across scenarios.

### Wind curtailment and lost load

To calculate wind curtailment in the optimization, we created an elastic demand variable with a zero cost to “absorb” wind overproduction. In contrast, the lost load is defined by the ratio (in percentages) between the energy (in GWh) that the system was not able to supply to satisfy the demand and the total demand (in GWh). Fig. 5 shows the cumulative distribution results for lost load and wind curtailment. The figure shows that all of the scenarios meet load 99% of the time, as we developed them to provide approximately the same reliability levels, measured by lost load, as those in the baseline scenario. The highest lost load levels occur only when the system faces a sequence of seasons with low wind speeds and little precipitation in the “Wind39” scenario.

The probability of wasting energy through wind curtailments is higher in the “Wind39” and “COD retirement” scenarios because of the higher wind penetration. The simulation results indicate some level of wind curtailment 40% of the time in these scenarios. Wind curtailment typically happens during the period of low loads, high wind speed seasons, and when the reservoirs are already filled and there is no more capacity to store water. The baseline and “Wind27” scenarios have similar empirical distributions for wind curtailment. For those scenarios, the energy curtailment occurs 13% of the time. The lower wind and hydropower penetration in the “Natural Gas” scenario leads to the lowest probability of wind curtailment across the expansion scenarios because of the higher capacity of dispatchable thermal power plants.

### Costs

For this analysis we estimated the costs of construction and operations of the system in the different scenarios. A summary and discussion of these results are available in the supporting information. The marginal cost of generation is a SDDP output defined by the change in the operating cost with respect to a change of 1 MWh in the load (reais/MWh or \$/MWh). Fig. 6 presents the load-weighted annual average marginal cost results from the 400 simulations for each scenario. The marginal cost projections show that the baseline has the lowest average load-weighted marginal cost at the end of the simulation period (around 200 reais/MWh; US\$56/MWh). The “Wind27” and “Natural Gas” scenarios have load-weighted average marginal costs of 240 reais/MWh (US\$67/MWh) and 275 reais/MWh (US\$77/MWh), respectively, by 2028. Note that the Brazilian government controls natural gas prices so we assumed that the marginal cost of operating new natural gas plants is 250 reais/MWh (US\$76/MWh), which is the same value projected by the EPE report files.

In contrast, the “Wind39” and “COD retirement” scenarios show a distinct load-weighted average marginal cost profile because of the higher wind penetration, especially in the second half of the period of analysis. After 2020, the dispatch of thermal power plants increases during the low wind season, increasing the marginal costs, especially during high load. By 2028, the load-weighted average marginal cost for the “Wind39” and “COD retirement” scenarios are above 300 reais/MWh (US\$70/MWh).

### Greenhouse gas emissions

In 2012, GHG emissions from thermal electricity generation in Brazil were estimated to 48.5 Tg of CO<sub>2</sub>eq, representing 3% of the total Brazilian emissions (1,488 Tg) (Ferreira et al., 2014). According to the Intended Nationally Determined Contributions (INDCs) presented to the United Nations Framework Convention on Climate Change (UNFCCC) Conference of the Parties (COP21) in Paris in December 2015 (Brazil, 2015), which have now been approved as the country’s first Nationally Determined Contributions (NDC), by 2030 Brazil intends to reduce annual GHG emissions by 900 Tg CO<sub>2</sub>eq from all sectors. Among others, one of the measures to achieve the emissions reduction

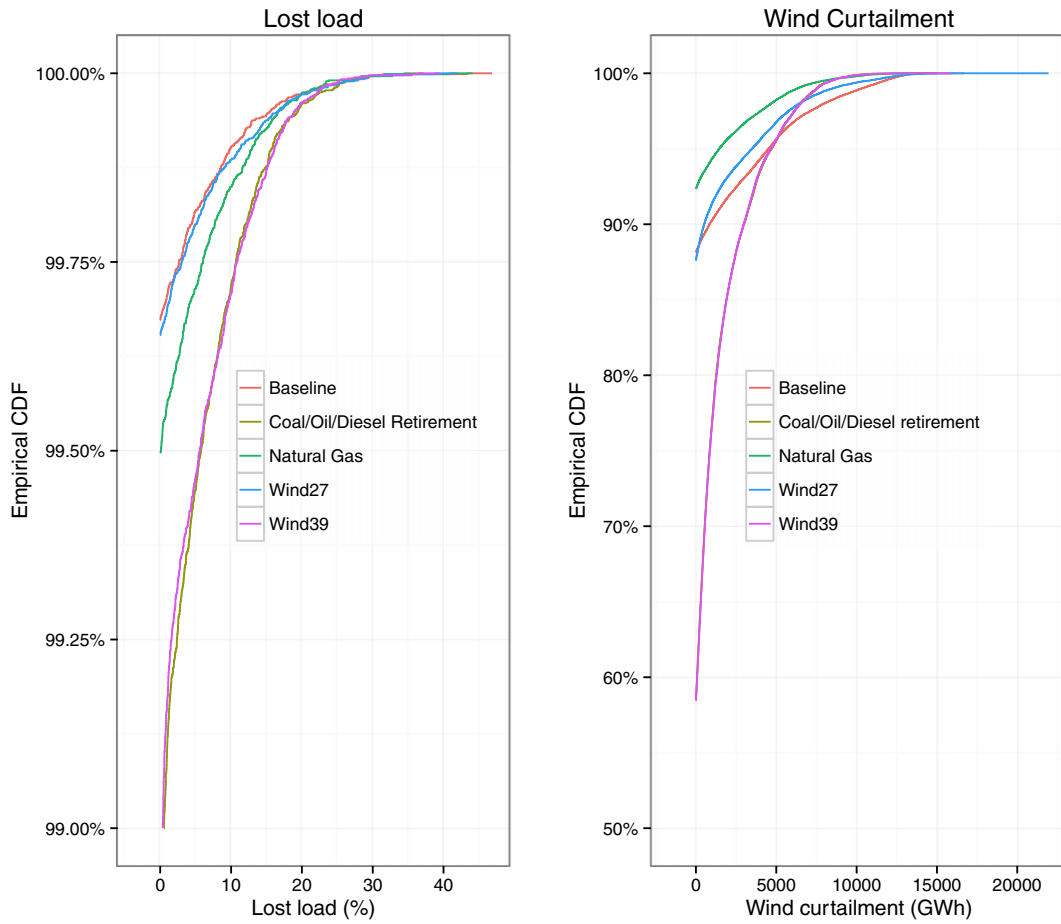


Fig. 5. Cumulative distribution functions (CDF) of lost load (as a percentage of the total demand) and wind curtailment (in GWh) by scenario. The sample used to build the CDFs consists in the percentage of the lost load and wind energy curtailed in each month considering the 400 simulations.

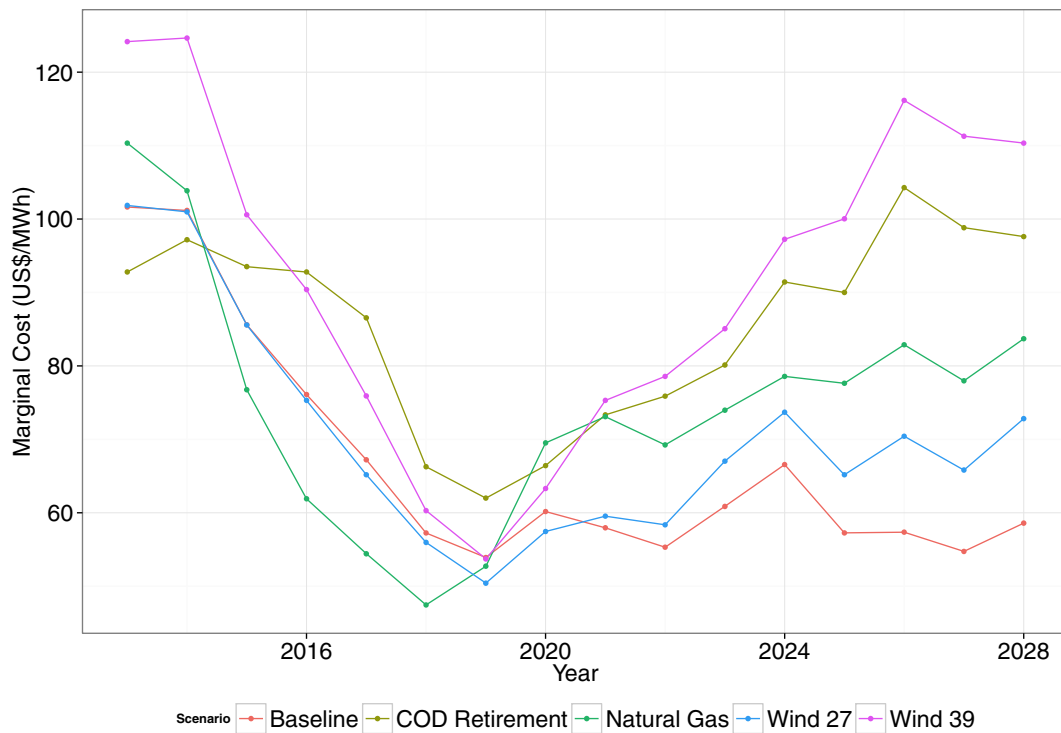


Fig. 6. Load-weighted average annual marginal costs for each scenario. To convert Reais to US\$, we used the May 2016 of 3.33 Reais/US\$.

target is an expansion of the share of wind, biomass, and solar in the power system to at least 23% (by capacity) by 2030.

Fig. 7 describes the total direct annual emissions from thermal power plants projected for each scenario, hereafter referred to as direct emissions. In 2014, average annual direct emissions total 47 Tg of CO<sub>2</sub>eq (95% CI: 21–99; this confidence interval, and others reported below, result from the 400 simulation of the operations of the system for each scenario. Such simulations account for stochasticity in wind and water inflows). In the baseline scenario, average direct emissions increase to 56 Tg of CO<sub>2</sub>eq (95% CI: 26–103) in 2028, when the share of wind, biomass, and solar in the total power capacity is 18%. This growth results from the increase in thermal generation observed in all capacity expansion scenarios (See Fig. 3, row 3).

The “Wind27”, “Wind39”, and “Natural Gas” scenarios also result in increased direct GHG emissions from power generation between 2014 and 2028, and by 2028 such emissions would be higher than in the baseline scenario. In 2028, direct emissions from the “Wind27” scenario total 63 Tg of CO<sub>2</sub>eq (95% CI: 30–107) when the share of non-hydro renewables is 30% of the total capacity. In the “Wind39” scenario, the higher non-hydro renewables share (40% of capacity excluding hydro) leads to even higher GHG emissions, estimated at 83 Tg of CO<sub>2</sub>eq (95% CI: 47–118) in 2028. These results indicate that direct GHG emissions from the Brazilian power system will likely increase by 2028 under government plans, even as Amazonia hydro capacity grows. Furthermore, replacing the Amazonian hydropower plants with wind could even increase direct emissions from the power sector. These increases in direct GHG emissions occur because more

thermal power generation is necessary to meet demand during dry and low wind speed seasons.

Not surprisingly, the “Natural Gas” scenario results in the highest direct annual GHG emissions (102 Tg of CO<sub>2</sub>eq in 2028; 95% CI: 60–159) due to the increase in thermal capacity. The “COD retirement” scenario evaluates the effect of replacing dirtier fossil fuel power plants by natural gas assuming the same level of wind penetration of the “Wind39” scenario. The exclusion of the dirtier fossil fuel power plants would reduce emissions in 2028 from 83 Tg of CO<sub>2</sub>eq (95% CI: 47–118) in the “Wind39” to 73 Tg of CO<sub>2</sub>eq (95% CI: 38–105) in the “COD retirement” scenario. Thus, GHG emissions from this scenario are still higher than in the baseline scenario. Those values do not include methane emissions from natural gas production, processing, and distribution, which have been shown to be significant (Pétron et al., 2012; Brandt et al., 2014).

While the box plot does not include potential emissions from Amazonian reservoirs, we included these emissions in the total emissions between 2013 and 2028 reported above the box blots in Fig. 7. Although there is substantial uncertainty in estimates of GHG emissions from Amazon reservoirs, de Faria et al., 2015 show that those emissions could be significant for specific hydropower plants. Using de Faria et al., 2015 results, we estimate that the new major hydropower plants in the Amazon would emit an additional 25 to 300 Tg of CO<sub>2</sub>eq into the atmosphere over the first 15 years of operation. While these emissions are still lower than the total direct emissions from fuel combustion, they are not insignificant and further demonstrate that emissions associated with power generation could continue to increase by 2028 even if new renewable capacity is added to the system. When taking into account

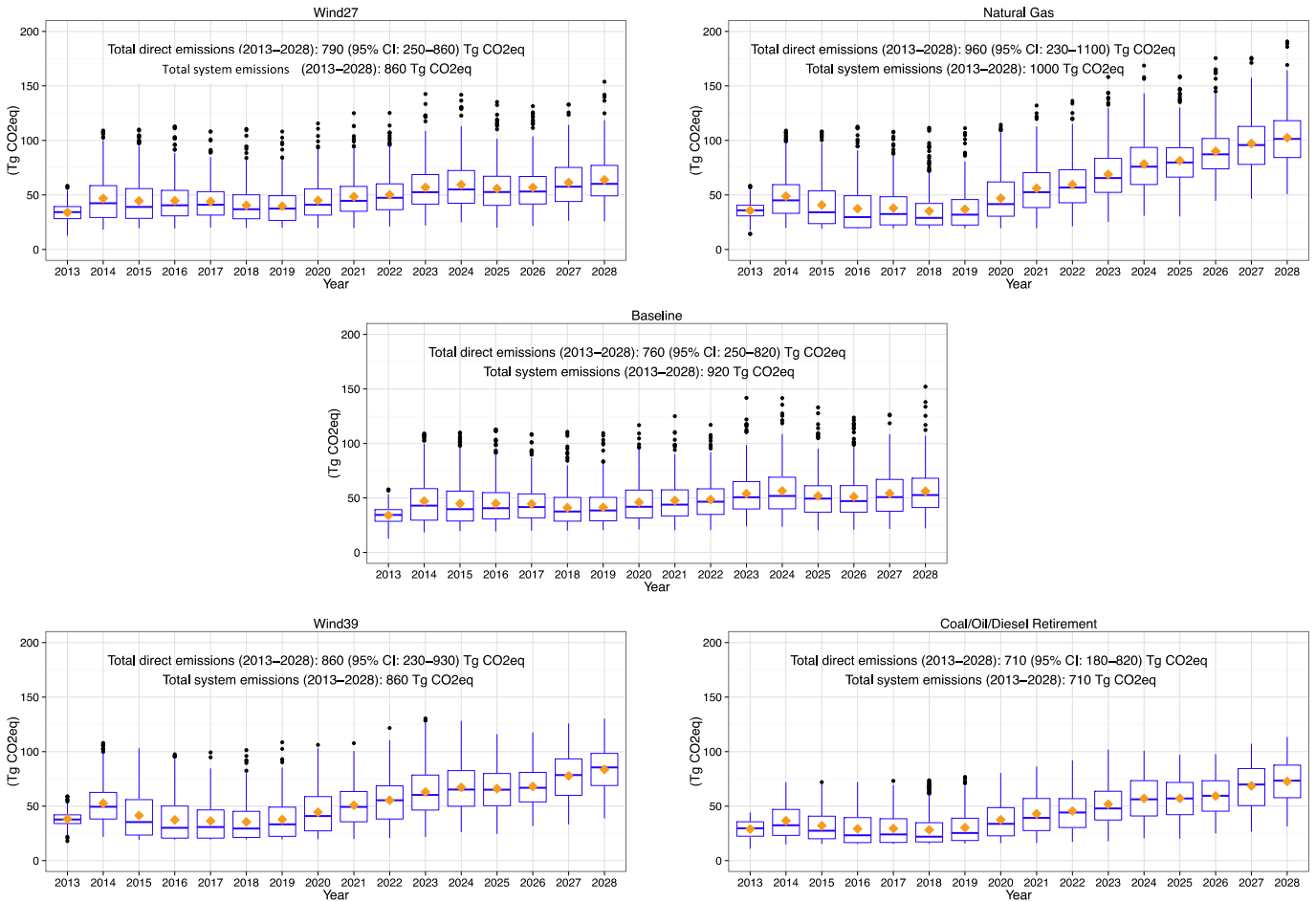


Fig. 7. Box-plots: annual direct greenhouse gas (GHG) emissions from power generation by scenario. Total system emissions include GHG emissions from new Amazon reservoirs plus total direct emissions in the study horizon. The baseline Amazon GHG emissions include the results from the eighteen hydropower plants defined by de Faria et al. (2015). “Wind27” and “Natural Gas” scenarios include only the emission from those eighteen hydropower plants build before 2020. Orange diamonds represent the average.

**Table 2**  
Land use requirements for each scenario by source (km<sup>2</sup>).

	Baseline	Wind27	Wind39/ COD Retirement <sup>a</sup>	Natural Gas
<i>Hydropower</i>				
Direct (EPE, 2015) <sup>b</sup>	9,000	1,700	0	1,700
Indirect Fthenakis and Kim (2009) <sup>c</sup>	34	27	15	29
<i>Natural Gas</i>				
Direct Fthenakis and Kim (2009)	115	130	137	205
Indirect Fthenakis and Kim (2009)	22	25	26	39
<i>Wind</i>				
Direct Fthenakis and Kim (2009)	1,386–2,217	2,212–3,538	4,219–6,751	1,386–2,217
Direct (Denholm et al., 2009 <sup>e</sup> )	3,900–6,500	7,800–13,000	12,000–20,000	3,900–6,500
Indirect Fthenakis and Kim (2009)	1–4	2–6	4–12	1–4
Total <sup>d</sup>	10,600–11,400	4,100–5,450	4,400–6,950	3,360–4,200

<sup>a</sup> In the case of the COD Retirement scenario, the replacement of Coal/Oil/Diesel power plants by natural gas is not included in the land use estimates, as we assume they would occupy the land currently used by replaced power plants.

<sup>b</sup> Based on information for each planned hydropower plant.

<sup>c</sup> Table S13 in the supporting information includes the land use rates from these studies.

<sup>d</sup> Total land transformation is calculated using wind direct land transformation by Fthenakis and Kim (2009).

the emissions from Amazonia reservoirs, the “COD retirement” scenario (which includes high wind penetration) has the lowest GHG emissions over the 15-year analysis period (710 Tg of CO<sub>2</sub>eq), followed by “Wind27” and “Wind39” (both with 860 Tg of CO<sub>2</sub>eq). The baseline scenario results in a total GHG emission of 920 Tg of CO<sub>2</sub>eq between 2013 and 2028. As expected, the “Natural Gas” scenario has the highest total system emissions (1,000 Tg of CO<sub>2</sub>eq).

#### Land use

Land use requirement for new power plants can serve as a proxy of non-climate related environmental and social impacts of generating capacity expansion. Table 2 describes the direct and indirect land transformation requirements for each scenario. Direct land use requirement for wind farms are a highly uncertain and vary substantially according to site-specific characteristics and estimation method. Different units have been used to report land use requirements for wind. For example, Denholm et al. (2009) reported land use in units of km<sup>2</sup>/MW, while Fthenakis and Kim (2009) reported them as m<sup>2</sup>/GWh. Using Denholm's number results in a higher estimate for the total land needed for wind in our scenarios, as shown in Table 2. Fthenakis and Kim (2009) assumed a typical capacity factor for wind farms to convert capacity to generation. The capacity factor of wind farms can vary substantially by location, which could be a bias in the number reported for wind farms by Fthenakis and Kim (2009) for this resource. Table S13 in the supporting information includes the land use rates used to calculate the values in Table 2.

The construction of all hydropower plants in the Amazon would require 9,000 km<sup>2</sup> (840 thousand soccer fields), resulting in a total land use requirement of approximately 10,500–11,400 km<sup>2</sup> in the baseline when accounting for all sources. The replacement of Amazon hydropower plants planned for construction after 2020 by wind farms

(Wind27) and thermal power plants (Natural Gas) would reduce land use by at least 50% and lead to total land use requirements of 4,000–5,500 and 3,400–4,200 km<sup>2</sup>, respectively. The replacement of all hydropower plants in the Amazon by wind farms would reduce land requirements to 4,400–7,000 km<sup>2</sup>.

#### Summary, policy implications and limitations

Table 3 summarizes the results for all the performance indicators for all scenarios included in this study. At the start of the analysis period, renewables account for 83% of installed capacity, though only 12% when excluding large hydropower plants. Except in the “Natural Gas” scenario, Table 3 shows that the proportion of renewable capacity in 2028 corresponds to 82% of the total capacity, a similar value compared to the renewables fraction in 2013. However, the share of renewables excluding large hydropower plants varies significantly across the expansion scenarios affecting the performance indicators.

Our results suggest that all capacity scenarios result in increased annual GHG emissions from power generation in 2028 compared to 2014, which highlight the challenge that Brazil will face in meeting its NDC under the Paris Agreement. Interestingly, the increase in emissions between 2014 and 2028 in the “Wind27” scenario is lower than in the “Wind39” scenario, even though wind is a lower percentage of the installed capacity in this scenario. As wind generation increases in our scenarios, so does cycling of thermal power plants, which increases the marginal cost and GHG emissions. A continued increase in emissions from the power sector seen in our scenarios suggests that emissions would have to decrease from other sectors for Brazil to meet reduction targets. It is important to note that the increased wind scenarios exclude an expansion of hydropower capacity in the Brazilian Amazon. If such resources were available in conjunction with increased wind, they could be used to balance wind variability, and potentially reduce the

**Table 3**  
Summary of performance indicators for all scenarios.

Performance indicators	Baseline	Wind27	Wind39	Natural Gas	Coal/Oil/Diesel retirement
Share of system capacity from renewables in 2028 (%)	82%	82%	82%	74%	82%
Share of system capacity from non-large hydro renewables in 2028 (%)	18%	30%	40%	19%	40%
Average marginal costs in 2028 (US\$/MWh)	54	67	101	77	90
Wind curtailment (ranking: 1 Higher; 4 Lower)	2	3	1	4	1
Average energy storage (in Dec. 2028, TWh)	95	102	140	85	140
Direct (Thermal) GHG emissions 2013–2028 (Tg CO <sub>2</sub> eq)	760	790	860	960	710
Hydropower GHG emissions 2013–2028 (Tg CO <sub>2</sub> eq)	160	60	0	60	0
% Change in average annual direct emissions between 2014 and 2028 <sup>a</sup>	+19%	+34%	+76%	+117%	+55%
Land use (km <sup>2</sup> )	10,600–11,400	4,100–5,450	4,400–6,950	3,360–4,200	4,400–6,950

<sup>a</sup> % change in annual average direct emissions calculated as (Average Emissions in 2028–Average Emissions in 2014)/Average Emissions in 2014.

emissions from cycling fossil-based power plants. However, the specific goal of this paper is to evaluate alternatives to expanded hydro capacity in the Amazon, as such expansion would be linked to negative environmental impacts (Latrubesse et al., 2017). Furthermore, even in the baseline scenario that includes the large expansion of Amazonian hydropower, emissions from power generation increase in 2028 compared to 2014, and such scenario would have larger emissions from land use transformation in the Amazon than the other scenarios. It is clear then, that in order to reduce emissions from power generation between 2014 and 2028 while also limiting the expansion Amazonian hydropower, Brazil would have to go beyond increasing wind generation. One option would be to replace part of the dirtier fossil fuel power plants with new natural gas or nuclear power plants. Another option would be to increase storage capacity by building low-impact storage reservoirs or assess the use of batteries and demand response mechanisms to reduce the thermal generation requirements during times of peak loads. Finally, demand-side interventions like improved use efficiency or load control can support emissions mitigation efforts.

Higher wind penetration contributes to increase average energy storage in the existing hydropower reservoirs but also increases the variability of supply at daily and seasonal scales. The wind variability problem should be more evident when modeling the system using a higher time resolution. We represented the daily variability using three load levels, which limits our ability to capture the high-frequency variability of wind or solar power output (Apt, 2007). Additionally, our simulations do not include transmission constraints, which would affect the dispatch of resources. Transmission investments are likely necessary to ensure that power from new non-large-hydro resources can be delivered to load centers like we assumed in this analysis. Finally, we did not use an optimal power flow model to evaluate the reliability of the power system accounting for steady state and stability issues. Such analysis is beyond the scope of this work. Future research should thus increase the resolution and simulate the system using hourly or minute time steps, as well as account for transmission constraints and power flow. An important pre-condition for modeling improvements is the access to better wind and solar data. We thus suggest future efforts should focus on creating a national database with high-resolution historical and simulated series of the wind speeds and energy output at higher temporal resolution than currently available.

This paper compares key performance indicators for an expanded power system in Brazil relying on different sources, including hydro-power plants in the Amazon, wind, or natural gas power plants. Although our scenarios are extreme as we assume complete replacement of one source by another, they have the advantage of underscoring the consequences of choosing one “winner” and its main effect on system operation and costs. The outcomes comparison in Table 3 suggests that the optimal energy mix is likely a hybrid of lower impact hydropower plants, wind and natural gas - more similar to scenario “Wind27” - than the baseline. Our work exemplifies how the simulation of the energy grid and the evaluation of performance indicators using several capacity expansion scenarios shed light on the consequences of adopting different strategies before the choice is made. Under a climate change scenario, Brazil and other countries should adopt this type of approach to improve low-carbon energy policy designs.

## Acknowledgments

CNPq (fellowship 202484/2011-4) supported this research. The RenewElec project and the Department of Engineering and Public Policy at Carnegie Mellon University also provided partial support. We thank Rafael Chabar, Mario Pereira Veiga, Raphael Kelman, Silvio Binato, Luis Carlos da Costa, Bernardo Bezerra, Celso Dalla'Orto, and Martha Carvalho from PSR (SDDP developer) for the valuable support and suggestions during the paper development. We also thank Dan Kirk-Davidoff and Steve Rose for helping with wind energy modeling. We thank CPFL Renovaveis and Raphael Ribas for providing real data

about Brazilian wind farms. The findings of this paper are the sole responsibility of the authors and do not represent the opinions of the funding sources.

## Appendix A. Supplementary data

Supplementary data to this article can be found online at <http://dx.doi.org/10.1016/j.esd.2017.08.001>.

## References

- Agencia Nacional de Energia Eletrica (Brazilian Electricity Agency). Electricity GENERATION DATABASE (Banco De Informacoes De Geraçao - BIG); 2015.
- Apt J. The spectrum of power from wind turbines. *J Power Sources* 2007;169:369–74.
- Apt J, Jaramillo P. Variable renewable energy and the electricity grid. Routledge; 2014.
- Barros N, Cole JJ, Tranvik LJ, Prairie YT, Bastviken D, Huszar VLM, et al. Carbon emission from hydroelectric reservoirs linked to reservoir age and latitude. *Nat Geosci* 2011;4:593–6.
- Bird L, Cochran J, Wang X. Wind and solar energy curtailment: experience and practices in the United States. National Renewable Energy Laboratory; 2014.
- Brandt AR, Heath GA, Kort EA, O'Sullivan F, Pétron G. Methane leaks from North American natural gas systems. *Science*; 2014.
- Brazil FRO. Federative Republic of Brazil intended nationally determined contribution. Fedferative Republic of Brazil; 2015.
- CCEE. Resultado consolidado dos leilões de energia; 2015.
- da Silva Soito JOL, Freitas MAV. Amazon and the expansion of hydropower in Brazil: vulnerability, impacts and possibilities for adaptation to global climate change. *Renew Sust Energ Rev* 2011;15:3165–77.
- de Faria FAM, Jaramillo P, Sawakuchi HO, Richey JE, Barros N. Estimating greenhouse gas emissions from future Amazonian hydroelectric reservoirs. *Environ Res Lett* 2015;10:1–13.
- Denholm P, Hand M, Jackson M, Ong S. Land-use requirements of modern wind power plants in the United States. NREL; 2009.
- dos Santos MA, Rosa LP, Sikar B, Sikar E, dos Santos EO. Gross greenhouse gas fluxes from hydro-power reservoir compared to thermo-power plants. *Energy Policy* 2006;34:481–8.
- EPE. Projeção da demanda de energia elétrica. Empresa de Pesquisa Energetica (EPE); 2014.
- EPE. Newave input files. Available at: <http://www.epe.gov.br/Estudos/Paginas/Plano%20Decenal%20de%20Energia%20E2%80%93%20PDE/EPEpublicaarquivosdoprogramaNewavedoPDE2023.aspx?CategoriaID=345>; 2015.
- Fearnside PM. Environmental impacts of Brazil's Tucuruí Dam: unlearned lessons for hydroelectric development in Amazonia. *Environ Manag* 2001;27:377–96.
- Fearnside PM. Brazil's Samuel Dam: lessons for hydroelectric development policy and the environment in Amazonia. *Environ Manag* 2005;35:1–19.
- Fearnside PM. Tropical hydropower in the clean development mechanism: Brazil's Santo Antônio dam as an example of the need for change. *Clim Chang* 2015;131:575–89.
- Ferreira AL, Tsai DS, da Cunha KB. Análise da evolução das emissões de gee no brasil (1990–2012): setor de energia, Observatório do Clima; 2014.
- Friedl G, Wuest AA. Disrupting biogeochemical cycles – consequences of damming. *Aquat Sci* 2002;64:55–65.
- Fthenakis V, Kim HC. Land use and electricity generation: a life-cycle analysis. *Renew Sust Energ Rev* 2009;13:1465–74.
- Gorenstin BG, M CN, da Costa JP, Pereira M. Stochastic optimization of a hydro-thermal system including network constraints. *IEEE Trans Power Syst* 2004:1–7.
- I.P.O.C.C. IPCC. Climate change 2014: synthesis report. Contribution of Working Groups I, II and III to the fifth assessment report of the Intergovernmental Panel on Climate Change. IPCC; 2014.
- Jackson S, Sleight A. Resettlement for China's Three Gorges Dam: socio-economic impact and institutional tensions. *Communis Post-Commun* 2000;33:223–41.
- Latrubesse EM, Arima EY, Dunne T, Park E, Baker VR, d'Horta FM, et al. Damming the rivers of the Amazon basin. *Nature* 2017;546:363–9.
- MME, EPE. Plano Decenal de Expansão de Energia; 2014.
- Moomaw W, Burgherr P, Heath G, Lenzen M, Nyboer J, Verbrugge A. IPCC special report on renewable energy sources and climate change mitigation; 2011.
- Oates DL, Jaramillo P. Production cost and air emissions impacts of coal cycling in power systems with large-scale wind penetration. *Environ Res Lett* 2013;8:024022.
- ONS. Consolidação da previsão de carga para a elaboração do programa mensal da operação energética. Operador Nacional do Sistema - ONS; 2010.
- Pereira M, Pinto L. Multi-stage stochastic optimization applied to energy planning. *Math Program* 1991;52:359–75.
- Pétron G, Frost G, Miller BR, Hirsch AI, Montzka SA, Karion A, et al. Hydrocarbon emissions characterization in the Colorado Front Range: a pilot study. *J Geophys Res* 2012;117:[n/a–n/a].
- PSR. SDDP Methodology Manual. Power Systems Research (PSR); 2014.
- Rose S, Apt J. What can reanalysis data tell us about wind power? *Renew Energy* 2015;83:963–9.
- Saha S, Moorathi S, Pan H-L, Wu X, Wang J, Nadiga S, et al. NCEP Climate Forecast System Reanalysis (CFSR) Selected Hourly Time-Series Products, January 1979 to December 2010; 2016.
- Tilt B, Braun Y, He D. Social impacts of large dam projects: a comparison of international case studies and implications for best practice. *J Environ Manag* 2009;90:S249–57.
- Tundisi JG, Matsumura-Tundisi T, Calijuri MC. Limnology and management of reservoirs in Brazil. *Comp Reserv Limnol Water Qual Manag* 1993;77:22–55.
- Tundisi JG, Rocha O. Reservoir management in South America. *Int J Water Resour Dev* 1998;14:141–55.